Journal of Inorganic and General Chemistry
ZAAC
Zeitschrift für anorganische und allgemeine Chemie
DOI: 10.1002/zaac.201900300
ARTICLE

Color-Changing Sparks from Rare Earth Metal Powders

Felix Lederle,[a,b] Jannis Koch,[c] Wolfgang Schade,[c,d] and Eike G. Hübner*[a,c]

Abstract. Commonly, sparks emit light according to the well-known black (gray) body radiation. Recently, we reported on color-changing sparks based on erbium powder, which switch their light emission between black body emission (surface combustion) and element-specific emission (vapor phase combustion). Herein, we investigated the spark formation from the adjacent rare-earth elements. The corresponding boiling points are significantly below (Yb, Sm, Tm) or above (Y, Lu) the boiling point of Er. While Yb and Sm evaporate too fast to form longer sparks, Y, Lu and Tm form color-changing sparks with varying length of the element-specific emission phase. The sparks were investigated by time-resolved emission spectroscopy, long-time exposures, and NIR/MIR imaging. The same basic pyrotechnic formulation containing one of these metal powders reveals a strongly differing burning behavior depending on the boiling point of the metal. The burning characteristics change from a green strobe (Yb) to intense colorful crackling (Tm) and finally a sparkling fountain with long-flying sparks (Lu, Y, Er).

Introduction

Usually, sparks formed by burning metal powders (e.g. Fe), alloys (e.g. ZrFe) or non-metals (e.g. charcoal) and inorganic compounds are colored according to the temperature of the hot burning particle.[1–4] The emitted light is well described by black/gray body radiation[5] which results in a very limited color space.[1] To achieve intense element-specific emission instead of element-independent black body emission, gas phase combustion of the particle is required. Consequently, the requirements to achieve element-specific coloring of sparks are:

(i) Intense emission from the metal or (high temperature stable) metal oxide.
(ii) Vapor phase combustion of the metal.

Both criteria limit the availability of appropriate elements. The first aspect can be checked by the flame/emission spectra of the elements. For the second aspect, *Glassman's* criterion as a critically discussed, yet in most cases correctly applicable rule predicts gas phase combustion if the boiling point of the element is lower than the boiling point of its reaction product (element oxide).[6,7] Additionally to *Glassman's* criterion, *Gordon* proposed various classes of burning particles with class A providing strongly visible gas phase combustion. The boiling point limit for substances in class A has been determined roughly around 1500 °C.[8]

In accordance with these criteria, broad and intensely colored sparks have been reported for ytterbium, samarium and tellurium as example.[9,10] As a drawback, these sparks are very short in length since gas phase combustion rapidly consumes large amounts of the material and the tellurium sparks hardly reach out of the flame which ignites them.[10]

Recently, we reported on color-changing sparks based on erbium powder. Erbium fulfills *Glassman's* criterion but its boiling point is substantially above *Gordon's* limit. As a consequence, these sparks switch their burning behavior between surface and gas phase combustion, accompanied by a color change from yellow to intense green.[10] Fortunately, the higher boiling point leads to long sparks suitable for spark generation in fountains.[10]

The burning behavior and radiation trace of isolated metal sparks has been analyzed in detail by *Dreizin*.[11] Although the elements differ strongly in detail, a typical radiation trace e.g. for aluminum is based on a first stage after ignition, a radiation jump indicates the second stage and subsequently a third less bright stage takes places which fades out until all material is consumed. At the end, particle explosion (branching, e.g. for zirconium) can take place.

This radiation trace can be brought in agreement with erbium sparks (Figure 1) which reveal a first stage based on black body emission, a short stage of bright element-specific emission just after the radiation jump and subsequently a long stage based on black body emission (and finally branching).[10] It must be noted, that for aluminum the radiation jump has

* Apl. Prof. Dr. E. G. Hübner
E-Mail: eike.huebner@tu-clausthal.de
[a] Institute of Organic Chemistry
Clausthal University of Technology
Leibnizstr. 6
38678 Clausthal-Zellerfeld, Germany
[b] Institute of Technical Chemistry
Clausthal University of Technology
Arnold-Sommerfeld-Str. 4
38678 Clausthal-Zellerfeld, Germany
[c] Fiber Optical Sensor Systems
Fraunhofer Heinrich Hertz Institute HHI
Am Stollen 19 H
38640 Goslar, Germany
[d] Institute of Energy Research and Physical Technologies
Clausthal University of Technology
Am Stollen 19 B
38640 Goslar, Germany
Supporting information for this article is available on the WWW under **http://dx.doi.org/10.1002/zaac.201900300** or from the author.

been brought in accordance with a temperature drop of the burning particle. Although it sounds contradictory on a first look, the burning particle forms aluminum-oxygen phases with a significantly reduced boiling point in comparison to the pure metal. The corresponding metal-oxygen phase consequently provides bright emission from a vapor-phase burning zone in case of Al. Consequently, even elements with higher boiling points than erbium may provide element-specifically emitting stages.

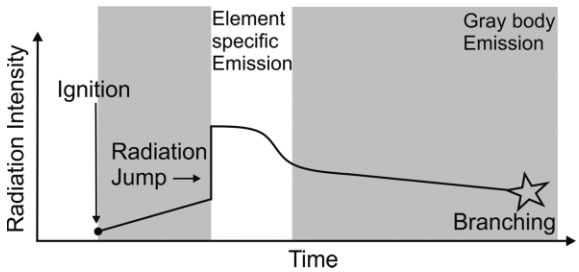

Figure 1. Typical radiation trace of sparks based on different burning stages given in literature[11] and element-specific colored stage observed for erbium.[10]

Recent work on pyrotechnic compositions includes a broad range of historically uncommon elements. *Jennings-White* gives a survey on potential candidates for pyrotechnic applications throughout the periodic Table[12] and recent examples include boron,[13–15] cesium compounds,[16,17] copper iodide[18] and copper complexes[19] as well as copper-based blue strobe compositions,[20,21] new formulations based on lithium,[22,23] and sodium salts,[24] detailed investigations of composition based on barium[25] and strontium[26] salts as well as calcium[27] and strontium tetrazolates,[28] and indium[29] metal. Rare earth metals were initially considered to be less useful until *Sturman* provided a detailed investigation of the emission from the atomic and monoxidic species of the rare earth elements in flames.[30] Furthermore, the application of some rare earth elements for element-specific colored sparks was suggested. Beginning in 2011, *Koch* presented the first investigations and pyrotechnic formulations based on Yb, Sm, Tm, and Eu with PTFE as oxidant.[9,31–33] As mentioned above, these formulations visibly emit short, but colorful pink or green sparks.[9]

Based on our observation of color-changing sparks from erbium powder ignited as isolated particles in a flame, here we investigated the coarse metal powders from Lu, Y, Sm, Tm and Yb concerning their spark formation upon ignition as loose powder in the flame phase. These rare-earth metals cover the range of boiling points clearly above (Y, Lu) and below (Sm, Yb, Tm) erbium (Table 1). Three more elements form color-changing sparks and we present pyrotechnic formulations thereof, which significantly change their burning behavior depending on the choice of the metal.

Results and Discussion

Elemental powders were obtained from rasping the rare-earth metals to coarse powder (ca. 100 µm) under inert conditions. The resulting particle size distribution is rather broad (Table 2), but sufficient to discuss the burning behavior of the metal powders. The rare earth powders have been passed into the invisible flame of a methan/air burner through a small tube and the resulting shower of sparks has been monitored by long time exposures (visible light, see Figure 2) and near/medium infrared (NIR/MIR, see Figure 3) imaging. A multimode glass fiber has been directed closely to the sparks to record time-resolved emission spectra with an integration time of 1 ms. Properties of the rare-earth metals are summarized in Table 1. The length and relative thickness of the sparks given in Table 2 were determined from photographic images.

The reactivity of the rare earth metals is roughly comparable according to their heat of combustion as well as electronegativity. All can be classified as highly reactive reaching very high flame temperatures. The boiling points of the metal oxides are located above the boiling point of the corresponding element, i.e. all rare earth metals discussed here fulfill *Glassman's* criterion. Consequently, they could provide element-specific emission from vapor phase combustion. It is remarkable, that the boiling points of the metal oxides are quite identical around 4000 °C. Consequently, the major difference of the rare earth metals discussed here is solely the boiling point of the metal. Beginning at 1200 °C (Yb) up to 3400 °C (Lu), the boiling point reaches ever closer to the boiling point of the oxide. According to *Gordon's* limit, Yb and Sm are below or at the edge for gas phase combustion, Tm and Er are above and Lu and Y far above the limit.

Erbium was investigated as reference first. The color-changing sparks are readily reproduced (Figure 2a) with Er obtained from a different supplier. The sparks fly rather long at the conditions applied here (Table 2) and the bright green phase is visible in the middle of the sparks for a length of roughly 20 % of the spark. The corresponding emission spectra (Figure 4a) show the expected stages of burning based on black body emission for the surface combustion (stage 1/3) and element-specific emission for the vapor phase combustion (stage 2).

Table 1. Physical and optical properties of the rare earth metals and oxides discussed here.

Element	ρ /g·cm^{-3} [34]	b.p. /°C [34]	ΔH_c /kJ·mol^{-1} [34]	b.p. stable oxide /°C [34]	Electronegativity [34]	Visible emission
Er	9.07	2868	–949.0	3000 [35] / 3920 [34]	1.24	beige//green
Lu	9.84	3402	–939.1	3980	1.00	white//pale green
Y	4.47	3345	–952.7	4300	1.22	light beige//red
Sm	7.52	1794	–911.5	3780	1.17	red [25]
Tm	9.32	1950	–944.4	3945	1.25	gold//green
Yb	6.97	1196	–907.3	4070 [36] / 4300 [35]	1.10	green [25]

Table 2. Particle sizes and characteristics of sparks obtained by elemental rare-earth powders.

Powder	D [a] /µm		Spark length /cm	Rel. thickness	Dom. WL [e] /nm	Sp. purity [e] /%
Er	20–195		4.5–8 [b]	–	–	–
		stage 1:	1	1	584	63
		stage 2:	1	3–5	562	28
		stage 3:	2.5–6 [b]	1–2	584	63
Lu	44–167		4–14.5 [b]	–	–	–
		stage 1:	1.5–2	1	582	36
		stage 2:	0.5	2–4	563	34
					(508) [f]	(8) [f]
		stage 3:	2–12 [b]	2	582	36
Sm	24–99		–	–	607	38
Y	27–253		4–8 [b]	–	–	–
		stage 1:	1–1.5	1	583	60
		stage 2:	0.5 [c]	3–4	588 [c]	50 [c]
					(602) [f]	(67) [f]
		stage 3:	2.5–6 [b]	2	–	–
Tm	20–119		3.5–6 [b] [d]	–	–	–
		stage 1:	1–1.5	1	589	85
		stage 2:	1.5	2	552	30
		stage 3:	1–3 [b]	1	589	85
Yb	42–247		–	–	566	27

a) Approx. grain size measured by optical microscopy. b) Limited by branching. c) Slowly fades out into stage 3. d) Main fraction bursts into small sparks. e) Dominant wavelength (WL) and spectral (Sp) purity determined by emission spectroscopy and CIE 1931 diagram. f) Calculated from RGB values of the corona of the spark.

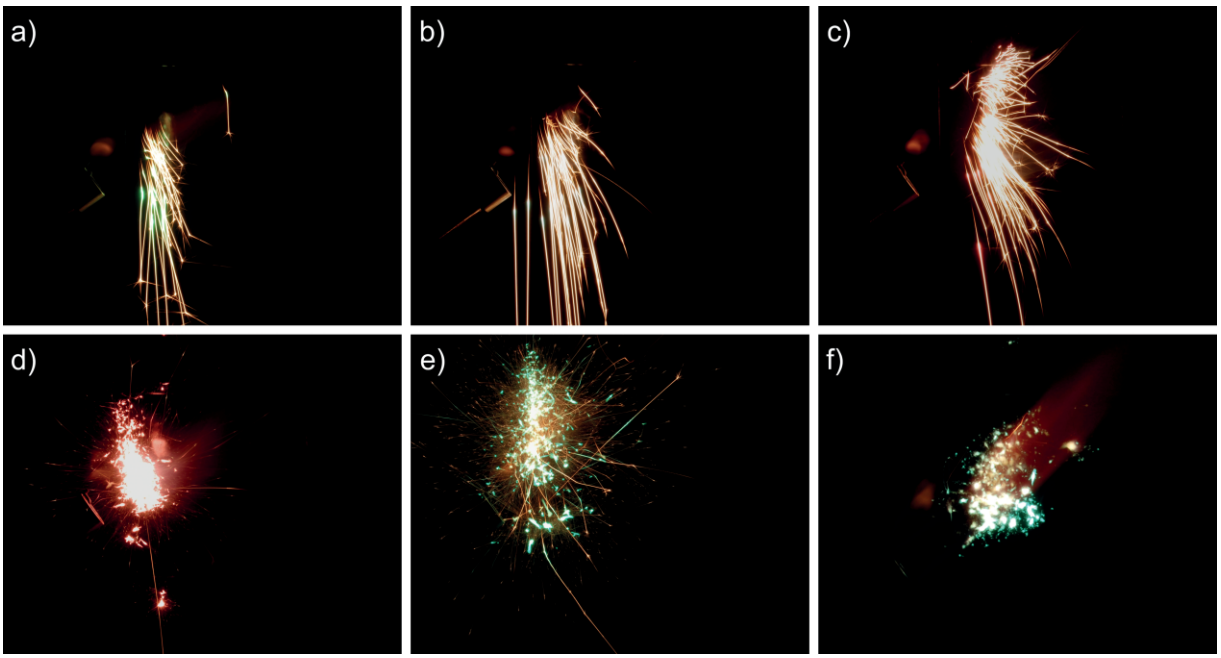

Figure 2. Long-time exposure images of sparks obtained from (a) erbium, (b) lutetium, (c) yttrium, (d) samarium, (e) thulium, and (f) ytterbium powder upon ignition of the rare earth metal powder in a gas flame.

Due to a more sensitive spectrometer setup and consequently a reduced integration time of 1 ms, vapor phase combustion stage 2 could be isolated sharper from the black body emission and the underlying background is reduced in comparison to our previous results.[10] The temperature of the spark at the surface combustion phase has been determined to 2680 K by *Planck* curve fit of the emission spectrum (Figure 4a). The emission spectrum of the vapor phase is in accordance with the flame spectrum of erbium salt solutions sprayed into an acetylene/oxygen flame given in literature.[37] The two intense and broad signals around 510 and 560 nm can be assigned to a set of emission bands from ErO located at 507 and 553–561 nm.[38] The data from the emission spectra were used to calculate the corresponding point in the CIE 1391 chromaticity diagram (Figure 5a) and to discuss the resulting dominant wavelength and spectral purity (Table 2). The color switches from basically yellow (surface combustion) to a significantly more green appearance (λ_{dom} = 562 nm) with a reduced spec-

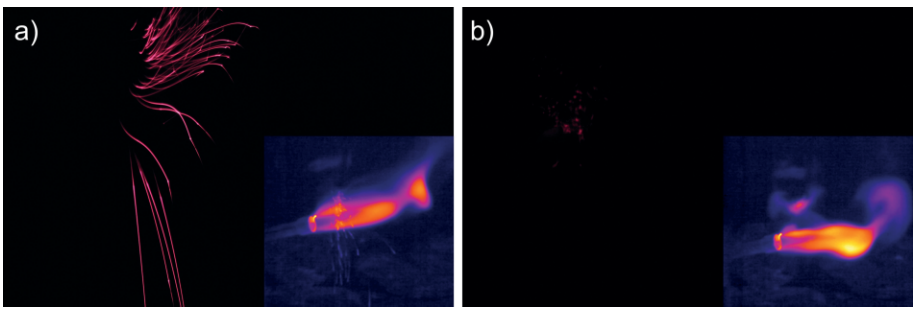

Figure 3. NIR (900–1100 nm) and MIR (insert, 8000–14 000 nm) images of sparks obtained from (a) yttrium and (b) samarium powder.

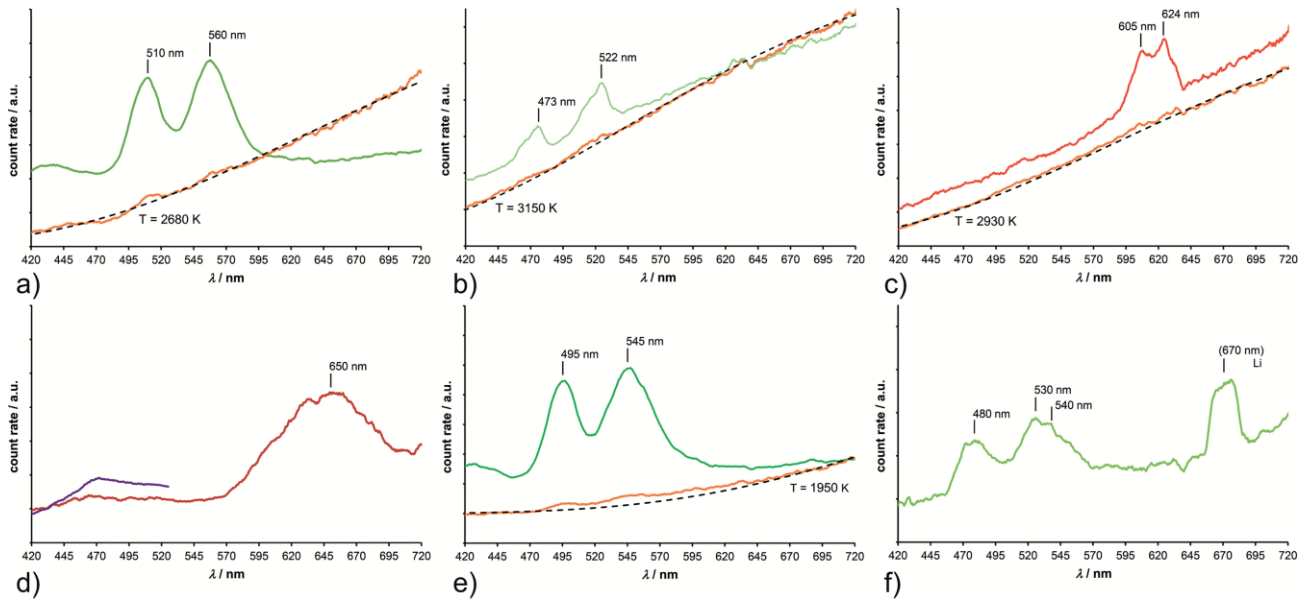

Figure 4. Emission spectra of sparks obtained (a) erbium, (b) lutetium, (c) yttrium, (d) samarium, (e) thulium, and (f) ytterbium powder upon ignition in the gas flame. Orange lines refer to surface combustion of stage 1/3 and differently colored lines to vapor phase combustion (stage 2 or the single stage observed for Sm and Yb). Dashed black lines represent fitted Planck curves.

tral purity which is explained by the superposition of black body emission and emission bands from ErO. Although the distance of two points in the CIE 1391 diagram is not an exact measure for the difference of two colors due to the concept of the diagram, we calculated the distance between the CIE coordinates of stage 1/3 and stage 2 as a rough estimate for visual difference of the burning stages. For Er, the difference is calculated to $d_{col} = 0.12$.

Lutetium is the highest boiling element of the rare earth metals investigated here. Looking at the long time exposure (Figure 2b) reveals long sparks with a very short and extremely bright stage 2 for the sparks formed from larger particles. At the first look, stage 2 might just be seen as a radiation jump. Looking at the sparks closer indicates vapor phase combustion, again, due to the increasing thickness of the spark during this short stage. Stage 2 is shorter in the case of Lu, and roughly half as long as in the case of Er, which is obviously explained by the high boiling point. For the same reason, the sparks are longer with a very long glowing stage 3. Additionally, branching is not as pronounced for Lu in comparison to Er. Sparks formation seems to be more sensitive to the particle size and only the largest particles (ca. 150 µm) form visibly differing stages. The spark temperature of stage 1/3 obtained from the *Planck* fit of the emission spectrum reveals a high burning temperature of 3150 K which is in accordance with the bright appearance. The spectrum of stage 2 unambiguously confirms gas phase combustion in by two broad signals at 473 and 522 nm (Figure 4b). The emission spectrum of the spark is in accordance with the flame spectra given in literature of Lu salt solutions[37] and the two signals can be assigned to LuO emission bands around 466–470 nm and 517–522 nm.[38] The emission spectra reveal a very strong underlying background of black body emission. This can be explained by the high temperature of the spark and strongly increasing intensity of the black body radiation with increasing temperature. Consequently, the color change from yellow/white to faint green/white is only weakly visible, indicated by a distance of the CIE color coordinates of $d_{col} = 0.06$ (Figure 5b). As an interesting aspect, it must be noted that the underlying black body radiation during the vapor phase combustion stage 2 seems to correspond to a lower temperature indicated by the decreased slope of the black body background (Figure 4b). This is in

accordance with the temperature drop during the radiation jump of aluminum sparks given by *Dreizin* and could be seen as a first indication for possible metal-oxygen phases with a reduced boiling point.

Yttrium has been described in literature to form white sparks.[39] The first look on the sparks confirms this observation. Analyzing the sparks more in detail reveals the same behavior as for the lutetium sparks. The larger particles, i.e. around 150–200 µm, show a clear change from yellow/white to a bright red upon ignition in the gas flame (Figure 2c). The bright red stage 2 is as short as in case of lutetium, which is in accordance with the comparable boiling points. It must be noted, that a red corona seems to remain around the yttrium sparks for a while if stage 2 was reached once, which is differing from Er and Lu sparks. The spark temperature during the black body emission stages has been derived to 2930 K, slightly lower than for Lu. The emission spectra of stage 2 show a significant underlying background of black body emission (Figure 4c). The two broad signals around 605 and 624 nm are in accordance with flame spectroscopy from Y[37] and are assigned to a series of YO emission bands at 597–600 nm and 613–617 nm.[38] As in the case of Lu, the intense underlying black body radiation weakens the visual appearance of the color change. This is confirmed by the small distance of the CIE color coordinates of d_{col} = 0.02 (Figure 5b). The corona of the Y sparks reveals a significantly more dominant coloring. Recalculating the RGB values from a spot of the corona in the photographic images to CIE coordinates visualizes the strong difference in the color of the spark and the corona (Figure 5b). The dominant wavelength of the corona is thus derived to 602 nm, which is in agreement with the YO emission bands. This matches with the expectation, since these CIE coordinates should correspond to the emission spectra cleared by the black body background. It has to be noted, that in the case of Y the color-change to red, which is part of the black body radiation, leads to a reduced apparent visibility in contrast to the color-change to green in the case of Er and Lu.

Taking the results from the high-boiling rare earth elements Er, Y and Lu together, in all cases color-changing sparks can be obtained and a color-change from basically yellow/white to green or red can be realized. All three elements form long-flying sparks, which frequently end with attractive branching. A higher boiling point of the metals shortens the bright and colored stage 2 and higher boiling metals require larger particle sizes to form color-changing sparks.

Samarium provides a significantly lower boiling point of 1800 °C. Compositions containing Sm and PTFE as oxidizer as well as burning Sm metal have been investigated in literature.[9,33] Images of the burning compositions given by *Koch* reveal some broad, short pink sparks to be emitted.[9] Here, we applied a coarse powder up to a particle size of 100 µm which bursts into an intense red flash upon contact with the gas flame (Figure 2d). The resulting "sparks" are deeply colored red which readily confirms gas phase combustion. The sparks are too short to be analyzed in terms of a spark length, most of the particles burned too fast and led to a nearly spherical flash on the photographic images at the conditions applied here. Some of the larger particles formed isolated sparks with a length of approx. 0.5 cm. The emission spectra revealed only a single burning stage with strong element-specific emission. The very broad signal around 650 nm is in agreement with the flame spectrum of Sm salts.[37] It is assigned to the intense series of bands emitted from SmO at 582–657 nm (Figure 4d).[38] Looking at the emission spectra of the sparks more closely reveals a weak emission band building up in the blue region. We were not able to obtain a sharper spectrum from the isolated sparks in the blue region to unambiguously identify the corresponding wavelength here, still it is likely to assign the very weak blue emission to line emission from atomic samarium.[30,38] The intense color of the bright samarium

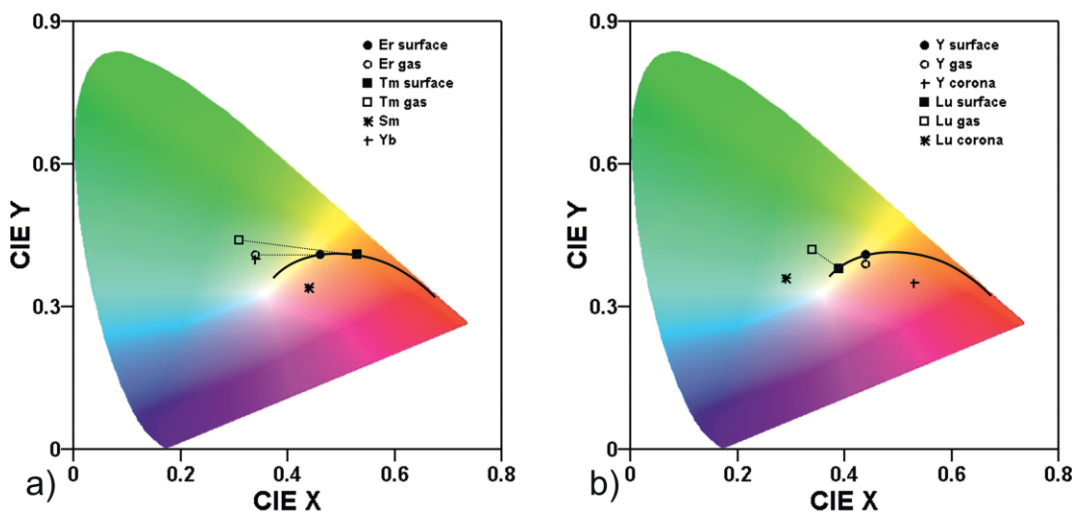

Figure 5. CIE 1931 chromaticity diagram of the sparks discussed here. "surface" refers to surface combustion (stage 1/3) and "gas" to vapor phase combustion. The black line represents the color of black body emitters (800–4200 K). CIE coordinates are derived from the emission spectra given in Figure 4 except for the corona of Lu and Y (calcd. from RGB values). Dotted lines represent the color change from surface to vapor phase combustion for the same material.

flashes strongly differing from the black body trace is reflected by the coordinates in the CIE diagram (Figure 5a). To compare the sparks from Sm solely based on vapor phase combustion to the sparks described before, IR spectroscopic images were taken (Figure 3, see Supporting Information for IR images of all other sparks discussed here). The yttrium sparks discussed above show an intense radiation trace on the NIR images (Figure 3a) which is in accordance with strong NIR emission from black body emission. The NIR images do not reveal a darkening during the vapor phase combustion in stage 2, which is in agreement with the strong underlying black body emission observed in the emission spectra. In contrast, the Sm flashes are hardly detectable on the NIR images (Figure 3b). Consequently we can conclude that only very weak black body emission is emitted, which matches with the expectation of pure vapor phase combustion. The results are confirmed in the MIR region, too (inserts in Figure 3) although the limited resolution of the MIR detector prohibits a detailed discussion. It must be noted, that rare earth oxides can provide strong emission in the IR region, which has been used for IR flare compositions based on Ytterbium.[40] In the case discussed here, the emission of the isolated particles is mainly based on the burning metal vapor phase (MO) and not its stable reaction product (M_2O_3) which is heated up from the burning composition. The foggy cloud visible in the MIR images on top of the gas flame (Figure 3b) could be caused from hot Sm_2O_3 formed during the combustion.

The boiling point of ytterbium is even lower in comparison to samarium. Consequently, the observations for Yb match with the results described for Sm and the coarse metal powder leads to bright green flashes upon contact with the flame (Figure 2f). Again, it is not possible to identify the length of isolated "sparks" under the conditions applied here. The emission spectra reveal only the element-specific emission of the vapor phase combustion (Figure 4f). Interestingly, the emission spectra of the isolated sparks show some significant differences to the spectra given by *Koch* for larger amounts of burning Yb metal[32] and differ from the flame spectra of Yb salt solutions.[37] Here, the spectra reveal only the characteristic set of two broad signals, which is quite similar in the case of Er, Lu and Yb. The two signals are assigned to emission bands of YbO at 474–484 nm and 544 nm.[38] Possibly, at 530 nm some contribution from an intense YbOH band at 533 can be seen.[38] This is in contrast to the spectra from *Koch*, which represent a large set of signals from atomic Yb emission. The isolated sparks of Sm and Yb show mainly the emission from SmO and YbO, respectively without significant contributions of atomic emission. The difference can be explained by the large amount of rare earth metal powder if burned in bulk, from which continuously metal vapor evaporates and saturates the flame phase. The emission spectra of Yb show a significant contamination with Li, indicated by the strong line at 670 nm. The Li atomic line in Yb spectra has been reported in literature,[32] too, and can be explained from residual Li which is a usual reductant (as elemental Li or Li-Mg alloy) in the preparation of the rare earth elements.[41] Usually, significant residues of the reductant can be found in the metals.[42] Looking at the photographic images given above, the typical red flame coloring from Li can be observed for Er, too. In the cases of elements forming longer sparks, the glass fiber was directed at the shower of sparks which is isolated from the gas flame and the Li emission is not detected. The CIE coordinates of the Yb flashes are in agreement with vapor phase combustion strongly differing from the black body trace (Figure 5a) and the NIR images again reveal the absence of significant IR emission (see Supporting Information).

Taking together the results from the low boiling elements Yb and Sm, the metal powders form more bright flashes than longer sparks upon contact with the flame. In both cases, vapor phase combustion with emission spectra based solely on the metal monoxide band emission is observed. The short spark formation can be compared to tellurium, which rapidly vaporizes,[10] too, but is not reactive enough to burn so violently.

Thulium finally provides a boiling point higher than Sm and Yb, yet lower than Er. Upon contact with the flame, intense and loud crackling during the combustion of the pure metal powder is observed. This is in agreement with crackling formulations of the rare earth elements with PTFE given by *Koch*.[9] A close-up view on the sparks (Figure 2e) reveals that the thulium particles burst into small pieces of which each forms a spark of a significant length. This is in agreement with the higher boiling point of Tm, which prohibits immediate vaporization. Although the sparks are smaller, since the particle burst into pieces, they reveal a very pronounced color change. The sparks consist of 3 stages of rather comparable length, i.e. the element-specifically colored stage 2 is roughly visible on 25 % of the total spark length (Table 2). The photographic images reveal a color change from gold to deep green. This is confirmed by the emission spectra (Figure 4e). The golden stage 1/3 is related to a spark temperature of comparably cold 1950 K, in agreement with the lower boiling point of Tm. The green stage 2 reveals a rather pure vapor phase spectrum with only weak underlying black body radiation. The two intense signals at 495 and 545 nm in the vapor phase spectrum are assigned to the set of monoxide emission bands of TmO at 481–494 nm and 533–556 nm.[38] Again, the spark spectra are solely based on the monoxide emission bands without contribution from atomic lines. Plotting the coordinates from the emission spectra into the CIE diagram visualizes the strong color change observed for Tm sparks (Figure 5a). The distance of the CIE color coordinates is calculated to $d_{col} = 0.22$. This is the largest color change for all sparks discussed here and can be explained by the low spark temperature leading to a more red stage 1/3 and low residual black body radiation during stage 2. The NIR image of Tm sparks (see Figure S4 of the supplementary material) represents the significant contribution of black body radiation in contrast to Sm and Yb. Overall, Tm is an interesting candidate for color changing sparks although its crackling burning behavior prohibits long-flying sparks.

The rare-earth metal powders were used to prepare fountains based on ammonium perchlorate (AP) and plasticized nitrocellulose (NC) as smokeless propellant.[10] The composition of the formulation has been kept constant at a ratio of 69 % (NC),

19 % (AP) and 12 % (rare earth metal powder). The mixture was loosely filled in paper tubes with 1 cm inner diameter and revealed a burn rate of 1.5–1.8 $mm \cdot s^{-1}$ in all cases. High resolution slow-motion (960 fps) videos of all experiments with this composition are given in the Supporting Information. The erbium-based composition ejects bright, branching sparks with a pronounced color change (Figure 6a) which is captured in the slow motion videos, too. The bright green stage 2 is visible as a brilliant flash in the trace of the spark. The formulation with Lu and Y ejects bright, long flying and branching sparks, too (Figure 6b, c). The color-change of the sparks is not represented in these sparkling fountains. In case of Lu, stage 2 is probably too short and visually too close to the extremely bright black body radiation of the hot sparks in stage 1/3. In the case of Y, the red stage is again too short, but the slow fading out of stage 2 discussed above visualized by a reddish corona around some larger Y sparks from coarser particles can be seen in the sparkling fountain (Figure 6c). In the case of the Sm based fountain, the metal powder burns too fast to be ejected as sparks. The flame color of the fountain is clearly red, but only single sparks occasionally reach out of the flame (Figure 6d). The fountain can be compared to the tellurium based formulation which rarely ejects isolated blue sparks.[10] The Yb based composition reveals a differing burning behavior, which is explained by the fast burning metal powder. Instead of ejecting sparks, the mixture repeatedly flashes in bright green (Figure 6f). The Yb powder is completely consumed before it reaches out of the tube, but provides sufficient light production to generate bright flashes. This can be seen as an interesting option for a strobe formulation, which is based on a different mechanism than usual strobe compositions.[2,3] Here, simply the fast burning particles lead to the visual appearance of repeated flashes. Finally, the thulium-based composition reveals intense crackling. The particles reach out of the tube and subsequently burst into pieces, which is accompanied by the crackling sound. The resulting fine sparks are emitted spherical around the bursting particle and a dense cloud of sparks is observed. Fortunately, the sparks still show the intense color-change as visualized in Figure 6e. Although this composition is not suited as an indoor fountain any longer, it may attract some interest as a very simple crackling composition.

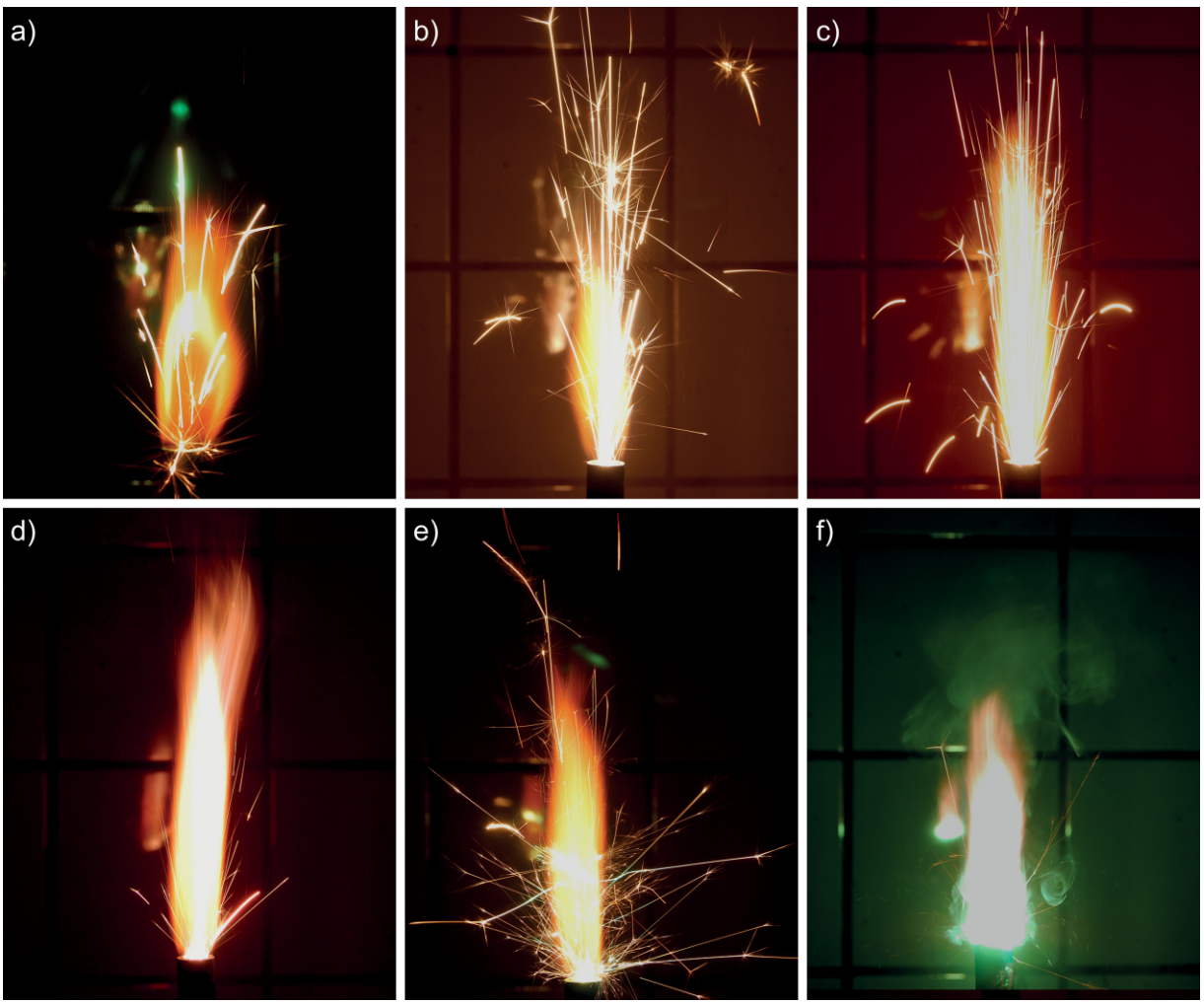

Figure 6. Photographic images (exposure time 30 ms) of smokeless ammonium perchlorate/nitrocellulose based fountains with (a) erbium, (b) lutetium, (c) yttrium, (d) samarium, (e) thulium, and (f) ytterbium powder.

Taking together the results of the AP/NC formulations, the rare earth metals provide very interesting burning characteristics. The simple choice of the metal allows distinguishing between strobe-like burning Yb, crackling Tm, or long-flying sparks based on Lu, Y and Er in exactly the same composition. In the view of color-changing sparks, erbium remains the best, if not only suitable choice.

Applying rare-earth metal powders to make an electric sparkler, well-known as popular indoor fireworks, is not straightforward. Usually, the electric sparklers are based on barium nitrate as oxidant and iron powder as sparkling fuel. The instability of the rare-earth metals towards water is one of the problems, since commonly dextrin/water (or gum arabic) is used as binder. Here, we transferred a standard electric sparkler formulation given by *Lancaster*[43] to non-protic conditions with NC as binder. NC was dissolved in butanone as moderately fast evaporating solvent. NC as binder is known to reduce the burn rate in comparison to inert binders,[44] which is explained by cooling of the reaction zone by enhanced gas production. Due to the high reactivity of the rare earth metals in comparison to iron, cooling from NC might be seen as advantageous in this case. Additionally, we replaced barium nitrate by strontium nitrate. Although strontium nitrate is rarely used, the reduced exothermicity of $Sr(NO_3)_2$ compositions in comparison to similar $Ba(NO_3)_2$ compositions was applied to compensate for the high energy release from the rare earth metals.[45] The slightly hygroscopic nature of $Sr(NO_3)_2$ was not a problem in this case, since the rare earth containing sparklers were kept under a dry atmosphere. Since the non-aqueous conditions prohibit any dissolution of the nitrate, which usually improves the mixing process, $Sr(NO_3)_2$ was ball-milled to fine powder before use. Fine aluminum flakes were used as basic fuel according to the standard formulation and with the typical particle size of 40 µm, which prohibits visible spark formation from aluminum powder.[46] The slurry obtained from this formulation was found to be well-suited to coat iron rods (insert of Figure 7a). After drying, mechanically stable sparklers were obtained. The sparklers turned out to be hard to ignite. After heating the tip of the sparklers with a gas flame, the reaction proceeded very fast and the whole sparkler burned within a fraction of a second. Obviously, the hot burning rare earth metals led to a very fast burn rate of the sparkler formulation. Still, we were able to capture some photographic images (Figure 7). In agreement with the results of the smokeless fountains, the Sm based sparkler did not eject colored sparks, but an intense red flash is observed. The Y based sparkler burst into a dense cloud of long-flying sparks. The reaction was too fast to capture isolated sparks, but the overall appearance is comparable to the fountain discussed above. As reference, the same formulation was prepared with iron powder and led to a sluggishly burning sparkler slowly ejecting iron sparks. Overall, we conclude the sparkling formulations based on the rare earth metal powders to be far too reactive.

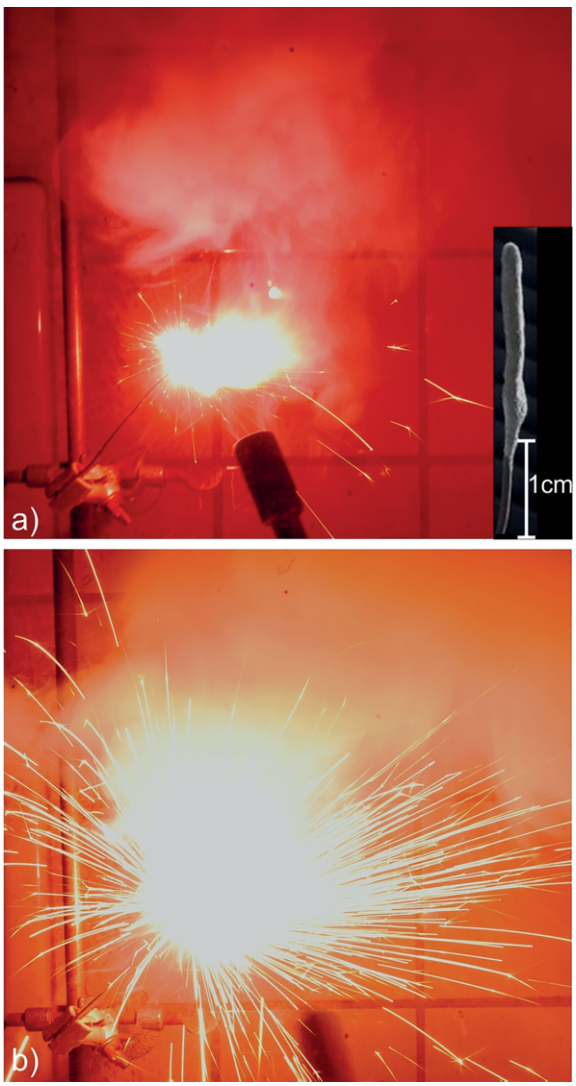

Figure 7. Photographic images of burning sparklers based on (a) samarium (insert: coated steel rod) and (b) yttrium powder.

Conclusions

Rare earth metals powders provide a unique burning behavior with intensely colored flames. All rare earth metals investigated here fulfill *Glassman's* criterion, although the boiling point of the highest boiling metals reaches quite close to the boiling point of the corresponding oxide. Consequently, we were able to detect colorful gas phase combustion for all sparks obtained from these metals on photographic images and the corresponding element-specific emission bands from the metal monoxides in the emission spectra. Since the boiling point of the metal oxides are rather close to each other, and the reactivity of the metals can be seen as quite identical, too, the main difference of the rare earth samples discussed here is the boiling point of the metal. In nice agreement with *Gordon's* limit we can classify the metals in roughly 3 groups. Yb and Sm, with a boiling point below or close to *Gordon's* limit, provide solely colorful vapor phase combustion. Lu and Y, with boiling points above 3000 °C, reveal mainly surface combustion which is based solely on black body emission and only a very short vapor phase combustion stage. Er and Tm, with a boiling point just between these two extrema, provide long

surface combustion and vapor phase combustion stages accompanied by a pronounced color change.

All sparks from the latter two groups reveal a general burning behavior based on a surface combustion stage 1 directly after ignition, a radiation jump to stage 2, which is characterized by vapor phase combustion and element-specific emission, respectively, and subsequently decreasing radiation intensity towards the second surface combustion phase finalized by branching.

Interestingly, all emission spectra of the isolated sparks are solely based on the metal monoxide emission bands and we did not detect significant emission from hot rare earth oxides (as stable reaction product) or from atomic emission lines. This is in contrast to the emission observed from burning larger amounts of the materials as bulk powder.

The rare earth metal powders were investigated concerning their applicability as sparkling fuel in NC/AP based fountains. Again, the boiling point of the metal dominates the resulting visual appearance and the same pyrotechnic composition reveals completely different effects depending on the metal. We found Yb and Sm to burn too fast to form longer sparks, as they hardly reach out of the tube although the particle size of the metal powders was coarse (above 100 µm). Instead, Yb with the lowest boiling point burns fast enough to form bright flashes and the composition appears as a green strobe. The Tm particles, with an increased boiling point, reach out of the tube and burst into smaller particles with an intense crackling sound. The resulting cloud of sparks represents an intense golden/green color change. Er, with a higher boiling point again, forms long-flying sparks with a bright green vapor phase combustion stage. Y and Lu, with the highest boiling points, lead to long-flying, brilliant white sparks finalized by branching while a colored vapor phase is virtually not visible.

Upcoming work will focus on alloys and intermetallic compounds instead of the pure elements.

Experimental Section

Caution! The rare earth metal powders investigated here are highly reactive and freshly prepared powders can be pyrophoric. Formulations given are meant for research purpose only and may be unstable. Mixtures containing ammonium perchlorate and nitrocellulose are potential explosives and should be handled with care. Rare earth metal containing formulations emit bright (UV) light and appropriate eye protection is required.

Ytterbium (99.95 %), yttrium (99.95 %), lutetium (99.95 %), erbium (99.9 %), thulium (99.95 %), and samarium (99.9 %) were obtained as block from Onyxmet and have been rasped to powder with a stainless-steel rasp under inert conditions. The resulting powder was carefully checked for the absence of steel particles and the absence of iron on the rare earth particles by energy dispersive X-ray spectroscopy (EDX). Strontium nitrate (Alfa Aesar) was ball-milled with a Retsch MM400 swing-mill and 3 steel balls (12.6 mm) for 2 min at 30 Hz in portions of 6 g (approx. 5 µm particle size). Stabilized and plasticized nitrocellulose (pyroflash Spezialeffekte) with an overall nitrogen content of 9.6 % was grinded to powder in a mortar with pestle. Ammonium perchlorate (Fluka), calcium carbonate (Sigma), aluminum flakes (40 micron, Merck), charcoal powder (50 micron, Fisher) and butanone (Sigma) were used as received.

Particle sizes of the rare earth metal powders were estimated by optical microscopy (Carl Zeiss Axioskop 20 equipped with Olympus DP10 digital camera). Long-time exposures (shutter speed 1 s) were taken with a digital camera (Nikon D40) referenced to the D65 white point. Due to strongly differing brightness of the sparks, varying aperture settings were used. Images were adjusted in overall brightness. No color corrections or tone adjustments were applied. An IR cut filter at 950 nm was used to visualize the NIR region from 900–1100 nm. MIR images (8000–14 000 nm) were taken with a Testo T885 IR camera. Emission spectrometric measurements were recorded with an AvaSpec-2048-USB2 spectrometer (Avantes) equipped with a 600 µm multimode glass fiber (Avantes FCB-UV/IR600-2-ME). The combination of spectrometer and fiber was calibrated with an incandescent tungsten lamp at 2715 K. All spectra were recorded with an integration time of 1 ms and spectra were recorded every 8 ms. Planck curve fits were prepared with OriginPro 2015. Chromaticity diagrams according to the CIE 1931 standard (Commission internationale de l'éclairage) were prepared with GoCIE v2[47] with CIE standard illuminant D65 as white reference point. All powders were passed into the centre of the invisible gas flame of a Teclu burner operated with methane through an aluminum tube from a distance of 20 cm.

Smokeless Fountain: A paper tube (5 cm length, 1 cm inner diameter, 2.5 mm wall thickness) was plugged with bentonite, which was strongly compactified by a plunger up to 2 cm from the top. Plastified nitrocellulose grinded to fine powder powder (1.10 g), ammonium perchlorate powder (0.30 g) and rare-earth metal powder (0.20 g) were mixed by repeated shifting on a paper sheet. The resulting mixture was inserted into the upper compartment of the paper tube until it was flush with the ending of the tube. The burn time is 11–13 s.

Electric Sparkler: Fine powder of strontium nitrate (1.66 g), aluminum powder (0.27 g) calcium carbonate (0.03 g), charcoal (0.02 g) and the rare-earth metal powder (1.00 g) were mixed by repeated shifting on a paper sheet. The mixture was filled in small tubes and soaked with a solution of nitrocellulose in 2-butanone (1.65 mL, c = 20 %). The slurry was stirred several minutes and subsequently steel rods (10 cm length, 1 mm diameter) were coated by repeated dipping into the mixture up to a total thickness of approx. 3 mm on a length of 2 cm. The rods were dried in a water-free atmosphere.

Supporting Information (see footnote on the first page of this article): Additional NIR/MIR images as well as microscopic images of all metal powders (pdf). High-resolution slow motion video compilation of the smokeless fountains containing all rare earth metal powders discussed here (mp4).

Acknowledgements

We sincerely thank *Dr. J. C. Namyslo* and *Birgit Wawrzinek* (Institute of Organic Chemistry, Clausthal University of Technology) for help with the swing mill. We thank *Werner Bischof* (Institute of Technical Chemistry, Clausthal University of Technology) for elemental analyses and *Simon Rauh* (Fraunhofer HHI, Goslar) for EDX measurements.

Keywords: Sparks; Rare earths; Lanthanides; Metal powders; Pyrotechnics

References

[1] B. J. Kosanke, K. L. Kosanke, C. Jennings-White, in: *Pyrotechnic Reference Series No. 4: Pyrotechnic Chemistry* (Eds.: K. L. Kosanke, B. J. Kosanke, B. Sturman, T. Shimizu, M. A. Wilson, I. von Maltitz, R. J. Hancox, N. Kubota, C. Jennings-White, D. Chapman, D. R. Dillehay, T. Smith, M. Podlesak), Journal of Pyrotechnics, Inc., Whitewater, **2004**, Chapter 13, pp. 1–14.
[2] T. Shimizu, *Fireworks The Art, Science and Technique*, 3rd ed., Pyrotechnica Publications, Austin, **1981**.
[3] J. A. Conkling, *Chemistry of Pyrotechnics*, Marcel Dekker, Inc., New York, **1985**.
[4] M. S. Russell, *The Chemistry of Fireworks*, 2nd ed., The Royal Society of Chemistry, Cambridge, **2009**.
[5] G. B. Rybicki, A. P. Lightman, *Radiative Processes in Astrophysics*, John Wiley & Sons, Inc., New York, **1979**, p. 22.
[6] I. Glassman, in: *Solid Propellant Rocket Research, Progress in Astronautics and Aeronautics* (Ed.: M. Summerfield), Academic Press, New York, **1960**, pp. 253–258.
[7] T. A. Steinberg, D. B. Wilson, *Combust. Flame* **1992**, *91*, 200–208.
[8] D. A. Gordon, in: *Solid Propellant Rocket Research, Progress in Astronautics and Aeronautics* (Ed.: M. Summerfield), Academic Press, New York, **1960**, pp. 271–278.
[9] E.-C. Koch, V. Weiser, E. Roth, S. Kelzenberg, in: Energetic Materials: Modelling, Simulation and Characterisation of Pyrotechnics, Propellants and Explosives, 42nd International Annual Conference of ICT, Conference Paper, Karlsruhe, **2011**, Chapter 1, pp. 1–11.
[10] F. Lederle, J. Koch, E. G. Hübner, *Eur. J. Inorg. Chem.* **2019**, 928–937.
[11] E. L. Dreizin, *Prog. Energy Combust. Sci.* **2000**, *26*, 57–78.
[12] C. Jennings-White, *Pyrotechnica* **1990**, *13*, 26–32.
[13] T. M. Klapötke, M. Rusan, V. Sproll, *Z. Anorg. Allg. Chem.* **2014**, *640*, 1892–1899.
[14] T. M. Klapötke, B. Krumm, M. Rusan, J. J. Sabatini, *Chem. Commun.* **2014**, *50*, 9581–9583.
[15] T. M. Klapötke, M. Rusan, V. Sproll, *Z. Anorg. Allg. Chem.* **2013**, *639*, 2433–2443.
[16] E.-C. Koch, *J. Pyrotech.* **2002**, 9–24.
[17] E.-C. Koch, V. Weiser, E. Roth, S. Knapp, T. M. Klapötke, S. Scheutzow in: Energetic Materials: Characterization and Modeling of Ignition Process, Reaction Behavior and Performance, 44th International Annual Conference of ICT, Conference Paper, Karlsruhe, **2013**, Chapter 21, pp. 1–9.
[18] T. M. Klapötke, M. Rusan, J. J. Sabatini, *Angew. Chem.* **2014**, *126*, 9820–9823; *Angew. Chem. Int. Ed.* **2014**, *53*, 9665–9668.
[19] O. S. Bushuyev, F. A. Arguelles, P. Brown, B. L. Weeks, L. J. Hope-Weeks, *Eur. J. Inorg. Chem.* **2011**, 4622–4625.
[20] D. Juknelevicius, T. M. Klapötke, A. Ramanavicius, *Propellants Explos. Pyrotech.* **2019**, *44*, 1466–1471.
[21] D. Juknelevicius, A. Dufter, M. Rusan, T. M. Klapötke, A. Ramanavicius, *Eur. J. Inorg. Chem.* **2017**, 1113–1119.
[22] A. M. W. Dufter, T. M. Klapötke, M. Rusan, J. Stierstorfer, *Z. Anorg. Allg. Chem.* **2019**. DOI: 10.1002/zaac.201900132.
[23] E.-C. Koch, *Propellants Explos. Pyrotech.* **2004**, *29*, 67–80.
[24] J. J. Sabatini, J. M. Raab, R. K. Hann Jr., C. T. Freeman, *Z. Anorg. Allg. Chem.* **2013**, *639*, 25–30.
[25] D. Juknelevicius, R. Kubilius, A. Ramanavicius, *Eur. J. Inorg. Chem.* **2015**, 5511–5515.
[26] D. Juknelevicius, L. Mikoliunaite, S. Sakirzanovas, R. Kubilius, A. Ramanavicius, *Z. Anorg. Allg. Chem.* **2014**, *640*, 2560–2565.
[27] E.-C. Koch, T. M. Klapötke, H. Radies, K. Lux, A. Hahma, *Z. Naturforsch. B* **2011**, *66*, 378–386.
[28] T. M. Klapötke, J. Stierstorfer, K. R. Tarantik, I. D. Thoma, *Z. Anorg. Allg. Chem.* **2008**, *634*, 2777–2784.
[29] J. Glück, T. M. Klapötke, T. Küblböck, *Z. Anorg. Allg. Chem.* **2019**, DOI: 10.1002/zaac.201900185.
[30] B. T. Sturman, *J. Pyrotech.* **1999**, 57–61.
[31] E.-C. Koch, V. Weiser, E. Roth, S. Knapp, J. van Lingen, J. Moorhoff, *J. Pyrotech.* **2012**, 3–9.
[32] E.-C. Koch, V. Weiser, E. Roth, S. Knapp, S. Kelzenberg, *Propellants Explos. Pyrotech.* **2012**, *37*, 9–11.
[33] E. Roth, S. Knapp, A. Raab, V. Weiser, E.-C. Koch, in: Energetic Materials: Characterization and Modeling of Ignition Process, Reaction Behavior and Performance, 44th International Annual Conference of ICT, Conference Paper, Karlsruhe, **2013**, Chapter 68, pp. 1–10.
[34] *CRC Handbook of Chemistry and Physics*, 84th ed. (Ed.: D. R. Lide), CRC Press LLC, Boca Raton, **2004**.
[35] A. Silverman, G. W. Morey, F. D. Rossini, *Natl. Res. Council Bull.* **1943**, *107*, 1–94.
[36] G. Benezech, J. P. Coutures, M. Foex, *J. Less-Common Met.* **1974**, *38*, 131–136.
[37] R. N. Kniseley, V. A. Fassel, C. C. Butler in: *Analytical Flame Spectroscopy* (Ed.: R. Mavrodineanu), Macmillan and Co. Ltd., London, **1970**, pp. 379–410.
[38] R. W. B. Pearse, A. G. Gaydon, *The Identification of Molecular Spectra*, 4th ed., Chapman and Hall, London, **1976**.
[39] K. L. Kosanke, B. J. Kosanke, B. T. Sturman, R. M. Winokur, *Pyrotechnic Reference Series No. 5: Encyclopedic Dictionary of Pyrotechnics Part 3*, PyroLabs, Inc., Whitewater, **2012**, p. 1045.
[40] E.-C. Koch, A. Hahma, *Z. Anorg. Allg. Chem.* **2012**, *638*, 721–724.
[41] T. Moeller, in: *Comprehensive Inorganic Chemistry* (Eds.: J. C. Bailar Jr., H. J. Emeléus, Sir R. Nyholm, A. F. Trotman-Dickenson), Pergamon Press, Oxford, **1973**.
[42] Z. Xiaowei, W. Zhiqiang, C. Dehong, L. Zongan, M. Ruiying, Y. Shihong, *Rare Met. Mater. Eng.* **2016**, *45*, 2793–2797.
[43] R. Lancaster, *Fireworks Principles and Practice*, 3rd ed., Chemical Publishing Co., Inc., New York, **1998**.
[44] D.-h. Ouyang, *Cent. Eur. J. Energ. Mater.* **2013**, *10*, 209–215.
[45] H. R. Pouretedal, S. Loh Mousavi, *J. Therm. Anal. Calorim.* **2018**, *132*, 1307–1315.
[46] K. L. Kosanke, B. J. Kosanke, in: *Selected Pyrotechnic Publications of K. L. and B. J. Kosanke*, Part 3, Journal of Pyrotechnics, Inc., Whitewater, **1996**, pp. 220–228.
[47] K. R. J. Thomas, GoCIE V2, Department of Chemistry, Indian Institute of Technology Roorkee, India, **2009**.

Received: November 18, 2019
Published Online: January 22, 2020

